https://doi.org/10.5194/tc-2020-112
Preprint. Discussion started: 25 May 2020

The Cryosphere Discussions

Sensitivity of the Antarctic ice sheets to the peak warming of Marine Isotope Stage 11

Martim Mas e Braga[1,2], Jorge Bernales[3], Matthias Prange[3], Arjen P. Stroeven[1,2], and Irina Rogozhina[3,4]

[1]Geomorphology & Glaciology, Department of Physical Geography, Stockholm University, Stockholm, Sweden
[2]Bolin Centre for Climate Research, Stockholm University, Stockholm, Sweden
[3]MARUM - Center for Marine Environmental Sciences, University of Bremen, Bremen, Germany
[4]Department of Geography, Norwegian University of Science and Technology, Trondheim, Norway

Correspondence: Martim Mas e Braga (martim.braga@natgeo.su.se)

Abstract. Studying the response of the Antarctic ice sheets to past climate conditions similar to the present day can provide important insights for understanding its current changes and help identify natural drivers of ice sheet retreat. The Marine Isotope Substage 11c (MIS11c) interglacial is one of the best candidates for an in-depth analysis given that at its later portion orbital parameters were close to our current interglacial. However, Antarctic ice core data indicate that although MIS11c CO_2 levels were close to Pre Industrial, warmer-than-present temperatures (of about 2°C) lasted for much longer than during other interglacials. Since the global mean sea level is thought to have been 6–13 m higher than today, there should have been some contribution from Antarctica. While substantial work has been conducted regarding the response of the Greenland Ice Sheet to the MIS11c climate, which is believed to have contributed with 3.9–7.0 m to global sea level, both configurations of the Antarctic ice sheets and their contribution to sea level rise remain poorly constrained. We use a numerical ice-sheet model to shed light on the response of the Antarctic ice sheets to MIS11c climate conditions obtained from a combination of a suite of Antarctic ice cores and the LR04 global stack of deep-sea sediment records and climate model outputs, while assessing the model sensitivity to the uncertainties in sea level reconstructions, ice sheet initial configuration, and multi-centennial climate variability. We found that the regional climate signal of the MIS11c peak warming in Antarctica captured by the ice core records is necessary for the recorded sea level highstand to be reproduced, and that warming length was more important than magnitude. However, there is a threshold for a West Antarctic Ice Sheet collapse that lies within an envelope of 1.6 and 2.1°C warmer-than-pre-industrial regional climate conditions. Sea level forcing and multi-centennial variability were found to have played virtually no role in driving ice sheet contraction, but the choice of initial configuration of the East Antarctic Ice Sheet provided a large source of uncertainty in the quantification of MIS11c Antarctic peak sea level contribution, which falls between 6.4 and 8.8 m.

1 Introduction

Marine Isotope Stage 11 stands out in the Quaternary history since one of its substages, substage 11c (hereafter MIS11c), was an interglacial period different from the preceding and subsequent interglacials of the Quaternary. First because it lasted for ca. 30 thousand years (kyr), between 425 and 395 thousand years ago (ka; Lisiecki and Raymo, 2005; Tzedakis et al., 2012),

https://doi.org/10.5194/tc-2020-112
Preprint. Discussion started: 25 May 2020


The Cryosphere Discussions
Open Access
EGU

thus making it the longest interglacial of the Quaternary. It also marked the transition from weaker to more pronounced glacial-interglacial cycles (EPICA Community Members, 2004). Its long duration is attributed to a modulation of the precession cycle, resulting in CO_2 levels that were high enough to suppress the cooling of the climate system due to the low eccentricity and thus reduced solar radiation (Hodell et al., 2000). Moreover, ocean sediment cores (e.g., Hodell et al., 2000) and climate models (e.g., Rachmayani et al., 2017) show that the MIS11c global overturning circulation was at an enhanced state, resulting in asynchronous warming of the southern and northern high latitudes (Steig and Alley, 2002). However, Dutton et al. (2015) surmise that, despite the fact that orbital parameters in MIS11c were almost identical to Present Day (PD) at its late stage (EPICA Community Members, 2004; Raynaud et al., 2005) and ice core reconstructions show the mean annual atmospheric temperatures over Antarctica to have been ca. 2°C warmer than Pre Industrial (PI) values, climate modelling experiments with realistic orbital and greenhouse gas forcings fail to fully capture this MIS11c warming, as they tend to underestimate climate variations during the interglacial (Milker et al., 2013; Kleinen et al., 2014).

A better understanding of the climate dynamics during the Quaternary interglacials, especially those that were warmer than today, is critical because they can help assess Earth's natural response to future environmental conditions (Capron et al., 2019). Among these periods, MIS 5e (also referred to as the Eemian, Last Interglacial, or LIG; Shackleton et al., 2003) was originally proposed to be a possible analogue for the future of our current interglacial (Kukla, 1997). More recently, MIS11c has been considered an even better candidate, since its orbital conditions were closest to PD (Berger and Loutre, 2003; Loutre and Berger, 2003; Raynaud et al., 2005). Furthermore, ice core evidence indicates that Termination V (i.e., the deglaciation that preceded MIS11) was quite similar to the last deglaciation in terms of rates of change in temperature and greenhouse gas concentrations (EPICA Community Members, 2004). The length of this unusual interglacial and the transition to stronger glacial-interglacial cycles seen in the recent geological record may have been triggered by a reduced stability of the West Antarctic Ice Sheet (WAIS, Fig. 1; Holden et al., 2011), and its long duration was shown to be key to the massive retreat of the Greenland Ice Sheet (GIS; Robinson et al., 2017). Elucidating the response of the Antarctic ice sheets (AIS) to past interglacials can also help identify various triggers that are able to drive ice sheet retreat. This is because each interglacial has its unique characteristics: for example, while MIS11c was longer than the LIG, the latter was significantly warmer (Lisiecki and Raymo, 2005; Dutton et al., 2015).

Compared to more recent interglacials such as the LIG, information for MIS11c is scanty (Dutton et al., 2015; Capron et al., 2019) and pertains primarily to the GIS. The MIS11c behaviour of the GIS, constrained through numerical modelling and empirical evidence, includes a strong retreat of its ice margin followed by vegetation expansion across southern Greenland (Willerslev et al., 2007; Reyes et al., 2014; Robinson et al., 2017; Rachmayani et al., 2017). Reyes et al. (2014) report a probable GIS contribution of 4.5 to 6 m of sea level rise based on simplified model simulations driven by MIS5e climate forcings that best fit their geological constraints for MIS11c, while Robinson et al. (2017) provide an estimated range of 3.9–7.0 m (and 6.1 m as their most likely value) of sea level rise based on targeted numerical simulations for MIS11c.

The MIS11c history of Antarctica is less constrained than that of Greenland. Whereas Raymo and Mitrovica (2012) consider that the WAIS had collapsed and that the East Antarctic Ice Sheet (EAIS, Fig. 1) provided a minor contribution based on their estimate of MIS11c global sea levels of 6 to 13 m above PD (Dutton et al., 2015), studies regarding the response of the

https://doi.org/10.5194/tc-2020-112
Preprint. Discussion started: 25 May 2020

AIS have been elusive. For example, sedimentary evidence has been inconclusive regarding the possibility of a collapse of the WAIS during certain Quaternary interglacials (Hillenbrand et al., 2002, 2009; Scherer, 2003), and only recently evidence for the instability of marine sectors of the EAIS has been provided (Wilson et al., 2018). Counter-intuitively, perhaps, the onshore dating of moraines in the Dry Valleys back to MIS11c is used to indirectly support regional ice sheet contraction, which would result in nearby open-water conditions and thus a source of moisture and enhanced precipitation, fueling local glacier advances (Swanger et al., 2017). Previous numerical modelling experiments that encompass MIS11 also do not show a consensus regarding AIS volume changes. For example, Sutter et al. (2019) report an increased ice volume variability from MIS11 onwards, caused by the stronger atmospheric and oceanic temperature variations, while Tigchelaar et al. (2018) only obtained significant volume changes during the last 800 kyr when increasing their ocean temperatures to unrealistically high values (i.e., applying a ca. 4° C surface warming anomaly to their experiments). Conversely, de Boer et al. (2013) report higher sea level contributions during MIS 15.5, 9, and 13, and weaker contributions during MIS 11 and 5.5.

Apart from the LIG, when studies acknowledge the possibility of a WAIS collapse (e.g., Hearty et al., 2007; Pollard and DeConto, 2009), the closest comparable period to MIS11c is the Pliocene, when the WAIS is also thought to have collapsed (Naish et al., 2009; Pollard and DeConto, 2009). However, Pliocene model results were shown to be highly dependent on the choice of climate and ice-sheet models (Dolan et al., 2018). Similarly, reconstructions from different ice cores do not fully agree on how temperature evolved during MIS11c. For example, the Vostok ice core surface air temperature reconstruction (Petit et al., 1999; Bazin et al., 2013) reveals a much shorter and weaker period of peak warming (about 2°C higher than PD around 410 ka) than that inferred from the EPICA Dome C (EDC; Jouzel et al., 2007) and Dome Fuji (DF; Uemura et al., 2018) ice cores, which have a lower uncertainty, and show a longer duration (ca. 15 kyr) of warmer-than-present temperatures (peaking at almost 4°C above PI around 407 ka for EDC, and 2.7 °C above PI at about 410 ka for DF, Fig. 1).

Given the absence of MIS11c-specific AIS model simulations, a dearth of information, and conflicting constraints on how Antarctica responded to this exceptionally long interglacial (Milker et al., 2013; Dutton et al., 2015), we here present the first AIS model reconstructions zooming in on the peak warming between 420 and 394 ka. We aim to reduce the current uncertainties in the AIS behaviour during MIS11c, specifically addressing the following questions:

1. How did the AIS respond to the warming of MIS11c? What are the uncertainties in the AIS minimum configuration, timing and potential sea level contribution?

2. What was the main driver of the changes in the AIS volume? Was it warming duration, peak temperature, or changes in precipitation? Are these drivers relevant to future ice sheet changes in the southern high latitudes?

For this purpose, we perform five ensembles of numerical simulations of the AIS to evaluate the importance for ice volume and extent of the differences in the signal intensity and structure of ice-core records, comparing to a reconstruction based on the LR04 stack of deep-sea sediment cores, uncertainties in sea level reconstructions, and uncertainties in the geometry of the AIS at the start of MIS11c.

https://doi.org/10.5194/tc-2020-112
Preprint. Discussion started: 25 May 2020

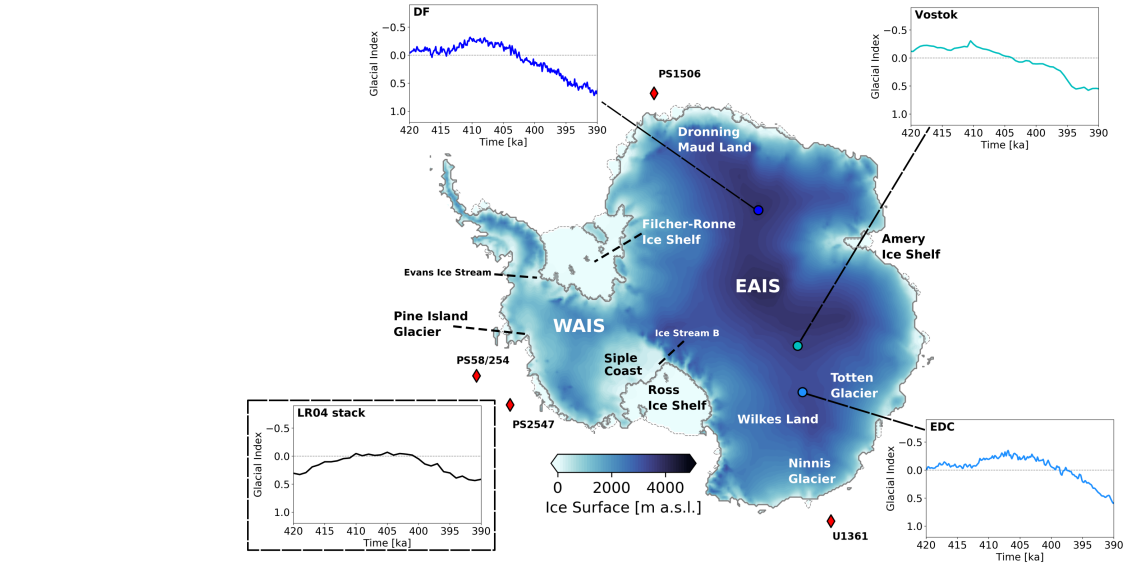

Figure 1. Surface topography of the AIS at the start of our experiments (420 ka, see Fig. 3d). The locations mentioned in the text, including the drilling sites of the ice (circles) and sediment (red diamonds) cores on and around Antarctica, are showcased. Also shown are the GI reconstructions for the adopted records (cf. Sect. 2.2, Table 2).

2 Methods

2.1 Ice-sheet model

For our experiments we employ the 3D thermomechanical polythermal ice-sheet model SICOPOLIS (Greve, 1997; Sato and Greve, 2012; Bernales et al., 2017a) with a 20 km horizontal grid resolution and 81 terrain-following layers in the vertical. It uses a one-layer enthalpy scheme that is able to correctly track the position of the cold-temperate transition in the thermal structure of a polythermal ice body (Greve and Blatter, 2016). For the basal melting of ice shelves, it adopts a calibration developed by Bernales et al. (2017b) to optimise a parameterisation based on Beckmann and Goosse (2003) and Martin et al. (2011), but with a quadratic dependence on temperature (as in Holland et al., 2008; Pollard and DeConto, 2012), which is able to respond to the variations in the Glacial Index (GI, Sect. 2.2; a description of our parameterisation is given in the supplementary material). The quadratic dependence on thermal forcing is inspired by Favier et al. (2019), who obtained results in good agreement with coupled ocean-ice shelf simulations. For glacial isostatic adjustment, we use a simple elastic lithosphere, relaxing asthenosphere (ELRA) model. We also use constant salinity since initial sensitivity tests using spatially variable salinity showed a negligibly small effect on the parameterised basal melting rates. The relevant parameters used in the modelling experiments are listed in Table 1.

All ensembles cover a period from 420 to 394 ka. To initialise the AIS, we first perform a thermal spin-up over a period of 195 kyr from 620 to 425 ka (i.e., apply a transient surface temperature signal from the EDC ice core (Jouzel et al., 2007) while

https://doi.org/10.5194/tc-2020-112
Preprint. Discussion started: 25 May 2020

Table 1. Main Parameters used in the experiments.

Parameter	Name	Value	Units
E	Enhancement Factor	1	
n	Glen's Flow Law Exponent	3	
p	Weertman's Law p exponent	3	
q	Weertman's Law q exponent	2	
τ	ELRA model time lag	1	kyr
D	ELRA model flexural rigidity	2.0×10^{25}	Nm
γ_{lr}	Lapse Rate Correction	8.0	$^{\circ}\mathrm{C\,km^{-1}}$
S_0	Sea water salinity	35	
ρ_{sw}	Sea water density	1028	$\mathrm{kg\,m^{-3}}$
ρ_{ice}	Ice density	910	$\mathrm{kg\,m^{-3}}$
c_{p0}	Ocean mixed layer specific heat capacity	3974	$\mathrm{J\,kg^{-1}\,K^{-1}}$
γ_T	Thermal change velocity	10^{-4}	$\mathrm{m\,s^{-1}}$
L_i	Ice heat capacity	3.35×10^5	$\mathrm{J\,kg^{-1}\,K^{-1}}$

keeping the ice sheet geometry constant at PD). We then let the AIS freely adjust for 5 kyr, between 425 and 420 ka, applying transient EDC forcing as a relaxation period. This is to avoid a shock in suddenly letting the topography freely evolve at the start of our simulations.

2.2 Climate forcing

In our effort to assess similarities and differences in existing paleoclimate reconstructions, and regional differences in the ice-core records, we perform an ensemble of simulations where each member is forced by a GI (see Eq. 1) derived from δD from ice cores, and δ^{18}O from the LR04 stack of deep-sea sediment cores (Fig. 2a; Petit et al., 2001; EPICA Community Members, 2004; Lisiecki and Raymo, 2005; Uemura et al., 2018). Since a fully coupled climate-ice sheet model run over 26 kyr is at present computationally challenging, an evaluation of possible scenarios for the peak-temperature response during MIS11c based on the paleoclimate signals from different ice sheet sectors can be a simpler, yet effective approach. The GI method is a way of weighting the contributions from interglacial (PI) and full glacial (Last Glacial Maximum; LGM) average states. It does so by rescaling a variable curve (usually temperature or isotope reconstructions from an ice or sediment record) based on reference PI and LGM values, which consider PI climate as $\mathrm{GI} = 0$ and LGM climate as $\mathrm{GI} = 1$ (Eq. 1):

$$GI(t) = \frac{\delta \mathrm{X}(t) - \delta \mathrm{X}_{\mathrm{PI}}}{\delta \mathrm{X}_{\mathrm{LGM}} - \delta \mathrm{X}_{\mathrm{PI}}} \tag{1}$$

https://doi.org/10.5194/tc-2020-112
Preprint. Discussion started: 25 May 2020


The Cryosphere Discussions

Table 2. Ice and sediment cores reference values used in Eq. (1).

Record	$\delta \mathrm{X}_{\mathrm{PI}}$ [‰]	$\delta \mathrm{X}_{\mathrm{LGM}}$ [‰]	Age (ka)	Age scale	Reference
EDC	-397.4	-449.3	24.0	EDC3	EPICA Community Members (2004)
DF	-425.3	-469.5	22.8	AICC2012	Uemura et al. (2018)
Vostok	-440.9	-488.3	24.4	GT4	Petit et al. (2001)
LR04	3.23	4.99	20.0	LR04	Lisiecki and Raymo (2005)

Where t is time, and X is Deuterium for the ice cores or ^{18}O for sediment cores. The value for $\delta \mathrm{X}_{\mathrm{PI}}$ was obtained as the average of the last 1000 years before 1850 CE, while $\delta \mathrm{X}_{\mathrm{LGM}}$ was taken as the minimum and maximum value for δD and δ^{18}O, respectively, between 19 and 26.5 ka (cf. Clark et al., 2009; Clason et al., 2014). For our two reference climate states (i.e., PI and LGM), we use the Community Climate System Model version 3 (CCSM3) PI time slice in Rachmayani et al. (2016), and the LGM time slice in Handiani et al. (2013), which used identical model versions and were run on the same platform. A brief assessment of the model biases against PD data is provided in the supplementary material. For further details the reader is referred to the respective original papers. The atmospheric and ocean temperature (T) fields at time t are reconstructed using:

$$T(t) = T_{PI} + GI(t) \cdot (T_{\mathrm{LGM}} - T_{\mathrm{PI}}) \tag{2}$$

while precipitation is reconstructed by an exponential function, to prevent negative values and also ensure a smooth transition between the PI and LGM states, using:

$$P(t) = {P_{\mathrm{PI}}}^{1-\mathrm{GI}(t)} \cdot {P_{\mathrm{LGM}}}^{\mathrm{GI}(t)} \tag{3}$$

The PI and LGM reference values (including the reference ages for the latter) for the three ice cores and the LR04 stack are summarised in Table 2, together with the respective age scales. The ensemble of simulations forced by different GI curves constitutes our core experiments and is termed CFEN (Climate Forcing Ensemble).

2.3 Sensitivity experiments

2.3.1 Uncertainties due to the GI scaling

Given the fact that different approaches have been used to transform the isotope curves into a GI, we assess the impact of such scaling by comparing the effect of changing the reference values for $\delta \mathrm{X}_{\mathrm{PI}}$ and $\delta \mathrm{X}_{\mathrm{LGM}}$. For the former, we tested using as reference the average of the last 10 kyr (rather than the 1000 years before 1850 CE), due to the fact that the temperature increase throughout the Holocene is inconsistent between ice and sediment cores (Fig. 2a). For the latter, we also treat $\delta \mathrm{X}_{\mathrm{LGM}}$ as the

https://doi.org/10.5194/tc-2020-112
Preprint. Discussion started: 25 May 2020

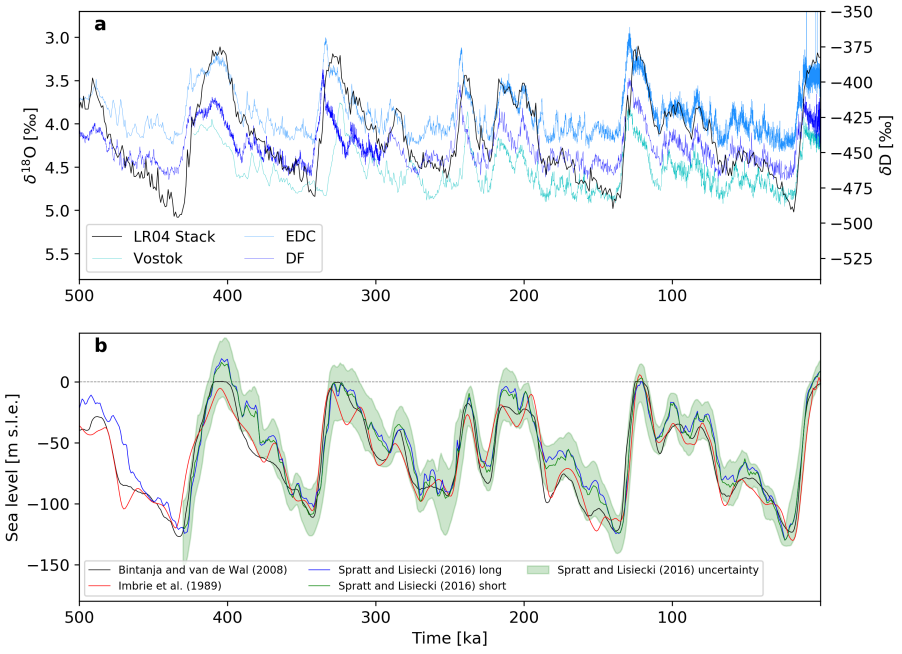

Figure 2. Reconstructions used in this study: (a) LR04 δ^{18}O (black) and ice-core δD [‰], and (b) global mean sea level anomaly relative to PI [meter sea level equivalent, m s.l.e.].

average (between 19 ka and 26.5 ka) instead of the peak value. We apply the different combinations of these references and their values to the EDC ice core δD and the LR04 stack δ^{18}O curves. For LR04 we only present the results for the sensitivity to the rescaling of $\delta^{18}\mathrm{O}_{\mathrm{PI}}$ since there was virtually no difference when changing the treatment for $\delta^{18}\mathrm{O}_{\mathrm{LGM}}$ (Supplementary Fig. S3). We call this ensemble the Scaling Sensitivity Ensemble (SSEN)

2.3.2 Impacts of multi-centennial variability

Given the different temporal resolutions of climate records, lower-resolution reconstructions such as LR04 and Vostok might not capture the impact of multi-centennial variability or shorter events, as do EDC and DF (Fig. 2a). Thus, we assess the potential effects of record data resolution and centennial time scale variability by applying 1, 3, and 5 kyr low-pass filters to the EDC ice core GI and forcing our model with the resulting smoothed GI curves. We then compare these three simulations to the unaltered EDC-derived ice sheet history, and call this ensemble the Resolution Sensitivity Ensemble (RSEN).

2.3.3 Uncertainties in sea level

Sea level plays an important role in determining the flotation of ice and the stresses at its marine margins. Uncertainties in global mean sea Level reconstructions are therefore a significant concern, and several studies have indeed focused on improving its estimates for the past millions of years (e.g., Imbrie et al., 1989; Bintanja and van de Wal, 2008; Spratt and Lisiecki, 2016,

https://doi.org/10.5194/tc-2020-112
Preprint. Discussion started: 25 May 2020

Fig. 2b). We evaluate the effect of using a particular sea level reconstruction on the evolution of the AIS by running an ensemble of simulations with EDC-based GI, where each member uses a different sea level reconstruction. Sea level curves included in this ensemble are three of the reconstructions presented by Spratt and Lisiecki (2016), termed "long" (i.e., uses records that extend as far back as 798 ka), "short" (uses records that extend at least until 430 ka), and the "upper uncertainty boundary" from their records, because we consider their lower uncertainty boundary to be satisfactorily covered by SPECMAP (Imbrie et al., 1989), which we include, and finally the reconstruction from Bintanja and van de Wal (2008). All these records are presented in Fig. 2b, and we call this ensemble, where we test for different sea level reconstructions, the Sea Level Sensitivity Ensemble (SLSEN).

2.3.4 Uncertainties in the initial ice sheet geometry

Similar studies that aim to assess AIS changes over (one or more) glacial and interglacial cycles often assume the PD geometry as a starting condition (e.g., Sutter et al., 2019; Tigchelaar et al., 2019; Albrecht et al., 2020), as has been done in our CFEN experiments. Although this has been loosely inferred from sedimentary (Capron et al., 2019) and ice-core (EPICA Community Members, 2004) proxy records, to our knowledge there is no direct evidence to support this (e.g., Swanger et al., 2017). Hence, we also perform an ensemble of simulations starting from distinct ice sheet geometries that are larger than PD, given the fact that at 420 ka the climate was transitioning to the interglacial. This allows for an evaluation of the influence of an initial configuration at 420 ka on the modelled retreat and advance of the AIS (including possible thresholds), and provides an uncertainty envelope in its potential sea level contribution based on this criterion. We call this the Starting Geometry Sensitivity Ensemble (SGSEN), and all its unique geometries are forced with the reconstructed climate forcings tested in CFEN.

In order to create a representative range of initial geometries, we vary the forcing conditions relative to the control run (i.e., temperature, precipitation, calving, and sub-ice-shelf melting) during the 425–420 ka relaxation. We use constant LGM temperature and LGM or PI precipitation fields during this period, as opposed to the transient GI approach of the control run. Table 3 summarises the different combinations used in creating each initial ice sheet geometry at 420 ka (labelled gmt1 to gmt3; Fig. 3). These different combinations allow the ice sheet to advance towards its intermediate-to-full glacial extent during a relatively short time, and their numbering (1 to 3) reflects an increasing areal extent relative to the 'control' run (Fig. 3d). Geometry 1 is generally more extensive and thinner than the control. Its grounding line advanced at the southern margin of the Filcher-Ronne Ice Shelf and at Siple Coast, but the ice sheet interior is on average 200 m thinner than the control and indeed up to 400 m thinner across particular regions such as the dome areas of the WAIS and Wilkes Land (Dome C). It is, however, about 200 m thicker at its fringes, which results in a gentler surface gradient towards the ice sheet margins. Geometries 2 and 3 show a more pronounced height difference and larger extent than the control run. They yield a slightly thinner ice sheet interior along its ice divides (less than 100 m), but thicker at the main drainage outlets (between 200 m in the interior and 400 m close to the former grounding lines). The gmt2 ice sheet is almost completely grounded across the Filchner-Ronne and Amery basins, with a reduced Ross Ice Shelf compared to gmt1. Finally, gmt3 has no prominent ice shelves, because the ice sheet becomes grounded across most of the domain.

https://doi.org/10.5194/tc-2020-112
Preprint. Discussion started: 25 May 2020

The Cryosphere Discussions
Open Access
EGU

Table 3. Experiments performed to create alternative initial geometries during the relaxation period between 425 ka and 420 ka. The experiments were designed to create increasingly larger ice sheet geometries, i.e., gmt1 larger than control but smaller and much smaller than gmt2 and gmt3, respectively (cf. Fig. 3).

Experiment	Temperature (atm/ocn)	Precipitation	Calving	Sub ice-shelf melting
control	transient	transient	On	On
gmt1	LGM	LGM	On	Off
gmt2	LGM	PI	On	Off
gmt3	LGM	PI	Off	On

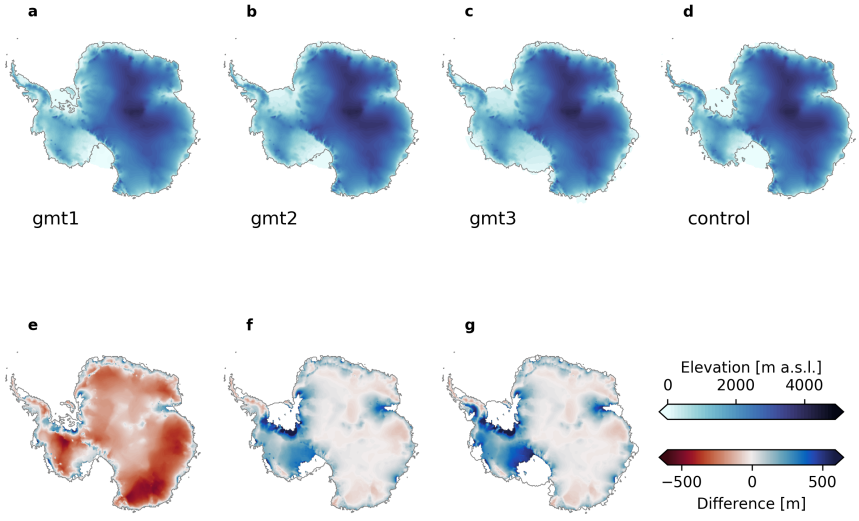

Figure 3. Different starting ice sheet geometries at 420 ka. (a-c) the different starting geometries corresponding to gmt1-gmt3 after 5kyr of relaxation following climate parameters given in Table 3; (d) original "control" conditions used for CFEN and SLSEN sensitivity analyses (Table 3). (e-g) difference maps between control (panel d) and the three alternative ice sheet geometries (respectively panels a-c). Differences are only shown where the ice is grounded in both geometries, and grey lines show the grounding lines in gmt1-3.

https://doi.org/10.5194/tc-2020-112
Preprint. Discussion started: 25 May 2020

3 Results

3.1 Climate forcing reconstructions

Considering the four adopted isotope curves (Fig. 1), although similar at first sight, the GI reconstructions are different from one another, and therefore offer a range of modelled ice-sheet responses. The LR04 GI reconstruction shows conditions close to PI for the warmest period of MIS11c (and colder-than-PI before and after), thus not showing a peak warming, or at least one that is warmer than PI (Fig. 6). Although the ice cores have similar ranges in GI values and similar overall aspects of the curves (and good covariance between EDC and DF; Uemura et al., 2018), they differ in key aspects (Fig. 1). The Vostok reconstruction starts at a warmer state than the others at 420 ka, has a modest peak warming at 410 ka, and then consistently declines towards a colder state (crossing the GI = 0 line at about 404 ka). The EDC reconstruction shows a mildly warmer-than-PI state at 420 ka, which persists until about 412 ka. Subsequently, the peak warming starts and persists (in a slightly warmer state than reconstructed with Vostok) until ca. 397 ka. Its rate of decline after about 404 ka is very similar to the Vostok and LR04 curves, although it is in a warmer state than the previous two. Finally, the DF reconstruction is somewhere in-between the other two ice cores (Fig. 1). It shows more stable conditions at the start (i.e., no pronounced warming), rising to a rather prolonged warming period similar in structure to the EDC reconstruction, but peaks at 410 ka, similar to the Vostok curve. Finally, its rate of decline is similar to the other cores and so it crosses PI values (GI = 0) later than the Vostok but earlier than the EDC curves, between 404 ka and 403 ka.

The ice sheet history for MIS11c using the LR04 forcing is clearly different from the others, because the ice sheet only becomes smaller than its initial state for a brief period of 1–2 kyr before 400 ka (Fig. 4). It is worth reminding that, in contrast to other members of CFEN, the LR04 curve starts with colder-than-PI conditions and does not become significantly warmer afterwards. It only shows a brief period of warmer conditions between 410 and 400 ka (Fig. 4a), resulting in the observed overall larger AIS (Fig. 4b). The ice core CFEN members yield lower ice volumes throughout all MIS11c (Fig. 4b), but with important variations. The Vostok-forced experiment, for example, introduces a faster ice loss at the beginning of the simulation period, when it shows a sudden warming (Fig. 4a). However, it recovers more quickly than the EDC and DF experiments as soon as the peak warming is over and the climate starts to shift back to PI conditions, without a WAIS collapse (Supplementary Fig. S4).

The members that result in a collapse of the WAIS (forced with the DF and EDC reconstructions) reveal slightly different responses. For example, the experiment forced by the EDC reconstruction shows an AIS volume reduction after a sudden warming at ca. 417 ka (Fig. 4), but the WAIS collapse is delayed until 410 ka, after a second short period with an increased warming rate, that leads up to the peak-warming of MIS11c. The DF experiment on the other hand is rather stable until ca. 412 ka, when the climate starts warming towards its peak. Most of the retreat seems to be triggered at times when the warming rate is strongest, as opposed to when the peak warming occurs.

For all ice core ensemble members, contraction of the AIS is already ongoing by 416 ka, and by 405 ka they are at, or close to, their minimum extents. In all CFEN simulations, ice sheet contraction is associated with strong basal melting close to ice shelf grounding lines, especially at Siple Coast at the Ross Ice Shelf and underneath the Evans Ice Stream at the Filchner-

https://doi.org/10.5194/tc-2020-112
Preprint. Discussion started: 25 May 2020

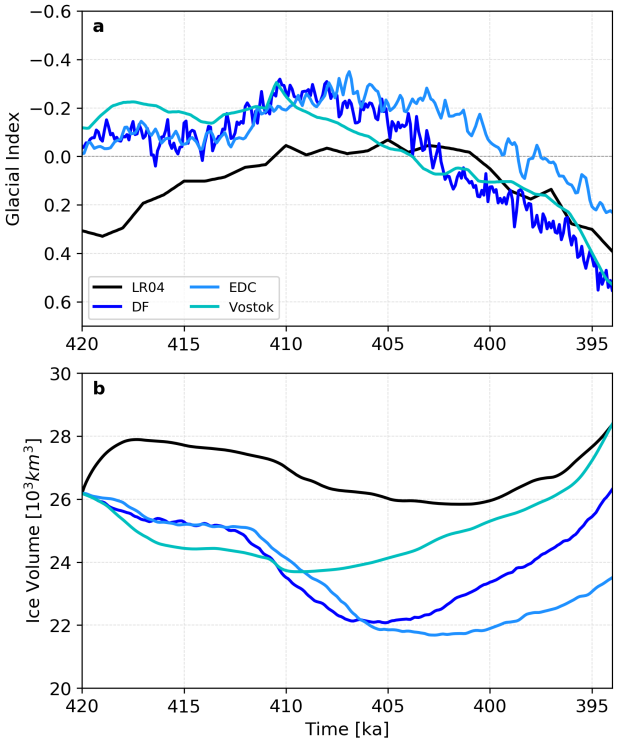

Figure 4. Sensitivity of AIS response to CFEN GI reconstructions during the peak warming between 420 ka and 394 ka. (a) GI reconstructions (cf. Fig. 2a). (b) Total ice volume [$10^3 \mathrm{km}^3$].

Ronne Ice Shelf (Fig. 5). These are caused by the combination of an increased warming of the ocean upper layer in these regions (Supplementary Fig. S5) and higher melt rates at the ice stream flux gates (Supplementary Fig. S2d). The same does not happen for the marine-based margin of western Dronning Maud Land, which shows more limited retreat during MIS11c than their western counterparts in the Weddell Sea region. Around most of the EAIS (except for the Amery Ice Shelf), either upper layer ocean temperatures or ice-shelf melt rates are not high enough to force grounding line retreat as strongly as in the aforementioned regions, and the relatively lower ice loss is dominated by surface ablation (Fig. 5).

3.2 Sensitivity to rescaling of the climate forcings

The different δ isotope reference values used for the SSEN experiments are shown in Table 4 (cf. Table 2). Using an LGM-averaged value results in a smaller ice sheet for the LR04 GI, while for the EDC GI it results in a slightly larger AIS than their correspondent CFEN experiments throughout the entire MIS11c (Fig. 6). This LR04-rescaled run, however, still does not produce significant AIS contraction compared to the other experiments, with an ice volume at 405 ka of ca. 10^6 km^3 less than its initial state (Fig. 6b). The warmer conditions resulting from the GI rescaling are still not enough to compensate for the initial growth caused by significantly colder conditions at 420 ka.

https://doi.org/10.5194/tc-2020-112
Preprint. Discussion started: 25 May 2020

The Cryosphere
Discussions
Open Access
EGU

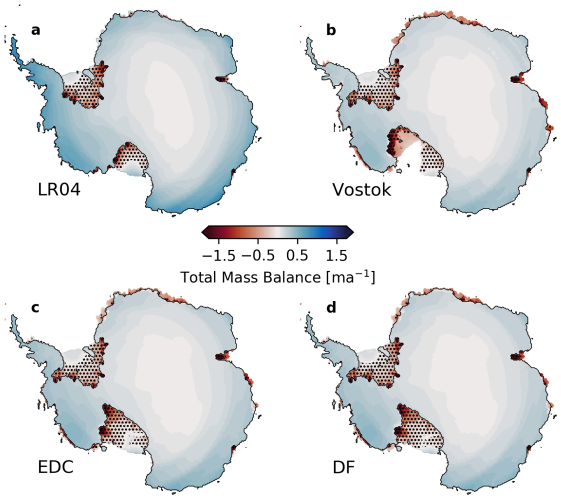

Figure 5. Total Mass Balance (i.e., ice shelf basal melting and surface mass balance combined, in ma^{-1}) at 416 ka for the CFEN simulations. Hatched areas show where basal melting dominates over surface mass balance.

Table 4. Different isotope values adopted for the GI rescaling procedure. *Hol* is the reference value produced by the average over the last 10 kyr (which replaces PI in Eq. 1 for the respective experiments), while *LGMavg* is the reference value obtained from the average between 26 and 19.5 ka (see Sect. 2.3.1).

Record	$\delta \mathrm{X}_{\mathrm{PI}}$ [‰]	$\delta \mathrm{X}_{\mathrm{Hol}}$ [‰]	$\delta \mathrm{X}_{\mathrm{LGM}}$ [‰]	$\delta \mathrm{X}_{\mathrm{LGMavg}}$ [‰]
EDC	-397.4	-394.6	-449.3	-442.3
LR04	3.23	3.33	4.99	4.85

Although differences in ice-sheet volumes exist between the different scaling strategies in the EDC-forced experiments, the resulting ice sheet histories are quite similar (Fig. 6b). Despite the ice-sheet volume at 405 ka being smaller in the run where both LGM and PI isotope values were applied differently to scale the EDC record (i.e., multi-millennial averages, see Sect. 2.3.1) than in the CFEN EDC-forced experiment, this difference amounts to ca. 0.6 m s.l.e., with only 0.1 m s.l.e. coming from the WAIS and the remainder coming from the EAIS (AIS sea level contribution, as well as separate contributions from EAIS and WAIS will be further discussed in Sect. 3.5 and thereafter). It is also important to keep in mind that using the last 10 kyr as reference for $\mathrm{GI} = 0$ is problematic due to the fact that the resulting GI for PI itself, which our reference fields are representative of, is much smaller than zero, which was the value it should have following the established routine for the derivation of paleoclimate conditions using a combination of GI and climate model time slices (e.g., Forsström et al., 2003;

https://doi.org/10.5194/tc-2020-112
Preprint. Discussion started: 25 May 2020

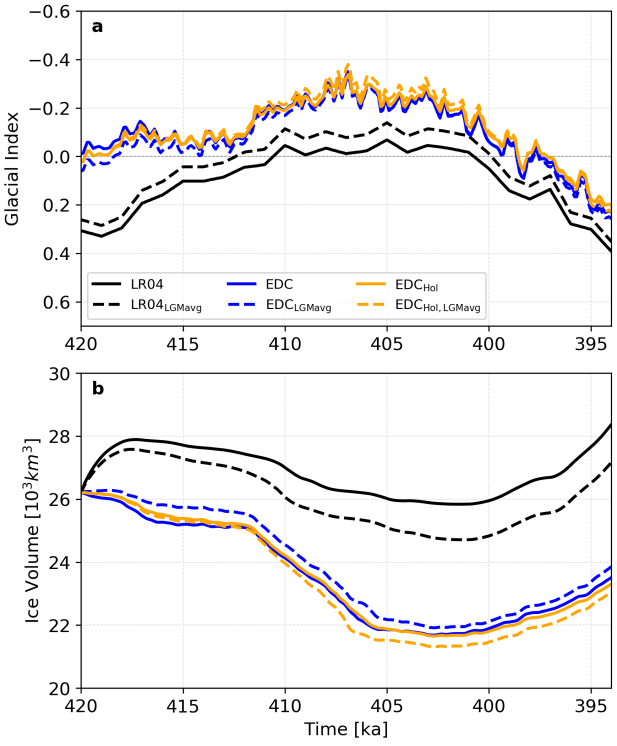

Figure 6. Sensitivity of AIS response to SSEN GI reconstructions during peak warming between 420 ka and 394 ka. "*Hol*" denotes the experiments where the last 10 kyr were used as opposed to the last 1 kyr, and "LGM$_{avg}$" denotes the experiments where the average over the LGM was taken as opposed to the peak value. (a) Differently scaled GI curves. (b) Total ice volume [10^3km^3].

Forsström and Greve, 2004; Greve, 2005; Clason et al., 2014). Consequently, the PI field has a stronger influence, producing an unrealistic forcing at time t that is warmer than expected.

3.3 Sensitivity to multi-centennial variability

Although the minimum volumes achieved by the filtered-GI experiments in RSEN are similar to the original ice sheet history obtained from the CFEN EDC-forced experiment, their individual trajectories are slightly different (Fig. 7). Ice sheet contraction and the timing at which each low-pass filter experiment reaches its minimum volume and starts its subsequent recovery are delayed compared to the original EDC forcing. The lag between the ice sheet histories increases with an increased filtering window. Whereas the 1 kyr low-pass experiment shows relatively small differences in the timing of the events compared to the CFEN EDC-forced run, the 3 and 5 kyr low-pass experiments show a significant delay in the ice sheet contraction (this is especially clear after 412 ka; Fig 7b). This effect seems to be non-physical, and a result of the delay introduced by the low-pass filter. While such delay prevents these results from being discussed in terms of absolute time, it still has implications for the impact of high-frequency variations. The 1 kyr low-pass GI is the only one that still preserves some higher-frequency variability,

https://doi.org/10.5194/tc-2020-112
Preprint. Discussion started: 25 May 2020

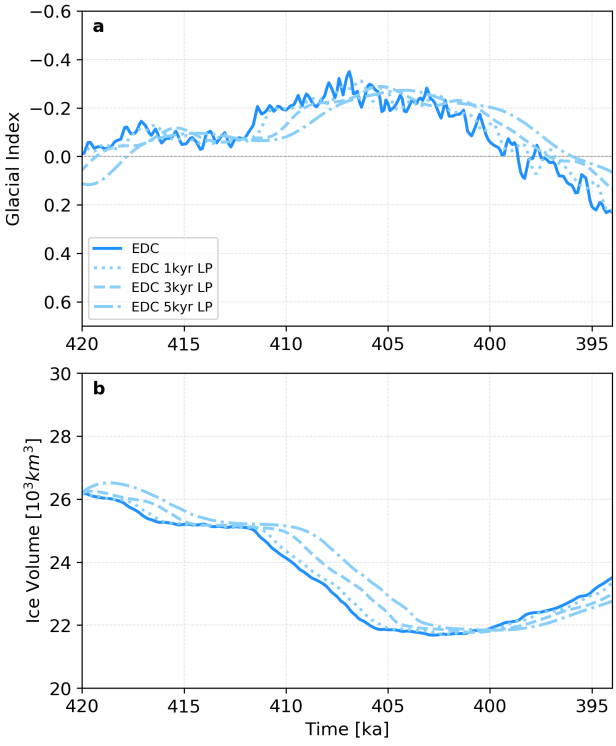

Figure 7. Sensitivity of AIS response to RSEN GI reconstructions during peak warming between 420 ka and 394 ka. (a) GI reconstructions. (b) Total ice volume [$10^3 \mathrm{km}^3$]. LP in the figure stands for "low-pass".

although its peaks are shifted or even in anti-phase with the original EDC GI series. This, however, appears to have little to no effect on the resulting ice sheet evolution, indicating that higher-frequency oscillations play a minor role in ice-sheet volume changes.

3.4 Sensitivity to sea level reconstructions

Although the range of global mean sea level reconstructions is wide (nearly reaching 60 m between 405 ka and 400 ka; Fig. 8a), the AIS response in terms of volume is remarkably similar for different sea level curves (Fig. 8b). The differences in sea level have largest impacts on the volumes of floating ice (Fig. 8c), directly reflecting their effect on the flotation of ice close to the grounding line. The SLSEN member with the highest sea level rise (i.e., the upper uncertainty boundary of Spratt and Lisiecki, 2016) deviates the most from the other members, especially in the portion of grounded ice being brought to flotation (Fig. 8c). However, the differences are not significant enough to yield substantially distinct ice volume changes (Fig. 8b).

https://doi.org/10.5194/tc-2020-112
Preprint. Discussion started: 25 May 2020

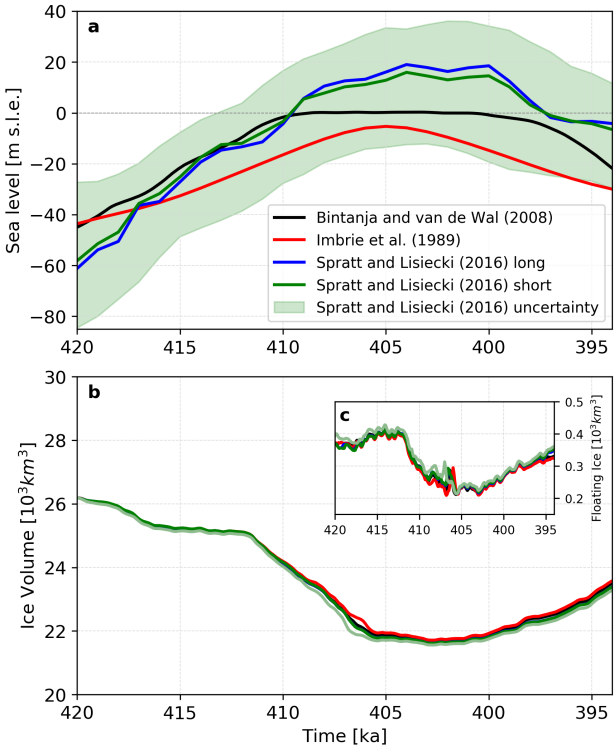

Figure 8. Sensitivity of AIS response to SLSEN reconstructions during peak warming between 420 ka and 394 ka. (a) records of global mean sea level relative to today [meter sea level equivalent, m s.l.e.] (cf. Fig. 2b). (b) Total ice volume [$10^3 \mathrm{km}^3$]; (c) Floating ice volume [$10^3 \mathrm{km}^3$].

3.5 Sensitivity to initial ice sheet geometry

In order to evaluate the uncertainty arising from the assumption of a PD-like initial ice sheet configuration, we perform a sensitivity experiment by running simulations starting from three alternative ice sheet geometries (Table 3) for those GI reconstructions indicating a WAIS collapse in CFEN, i.e., those forced by DF and EDC. We also include SSEN member forced by $\mathrm{EDC}_{\mathrm{Hol,LGMavg}}$ (cf. Table 4) in this analysis, since it attained a lower ice volume at 405 ka than any other member of CFEN, and thus provides an interesting end member for this ensemble. Finally, we also apply the same set of experiments to the Vostok GI reconstruction, in order to test whether a choice of alternative ice sheet geometries at 420 ka might trigger a WAIS collapse or enhance the response of the EAIS.

Looking at how the four initial geometries evolve under the four different climate forcings from the GI reconstructions (Fig. 9), it becomes clear that all members under the same climate forcing have a tendency to converge despite differing initial ice sheet configurations. Thus, the uncertainties in the minimum ice-sheet volumes (and consequently WAIS collapse) due to assumptions of starting geometry are rather small, with a spread between 1 and 1.1 m s.l.e. at 405 ka among the four

https://doi.org/10.5194/tc-2020-112
Preprint. Discussion started: 25 May 2020

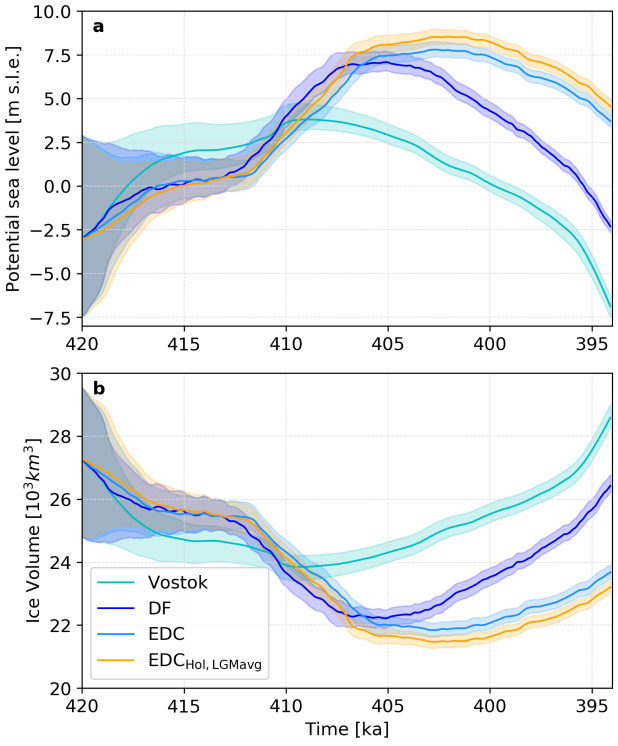

Figure 9. Sensitivity of the AIS response to CFEN GI reconstructions (Vostok, DF, EDC) and SSEN EDC$_{\mathrm{Hol,LGMavg}}$ between 420 and 394 ka with uncertainty bands from four distinct initial ice sheet starting geometries (Table 3). Contribution to (a) global mean sea level [m s.l.e.], and (b) total ice volume [$10^3 \mathrm{km}^3$]. Solid lines show the mean of each common-forcing ensemble member, while the color filling shows the spread given by the different starting geometries (cf. Fig. 3).

different members in SGSEN. The different ice sheet configurations also show similar rates of retreat, indicating that the ice sheet size does not affect its rate of contraction due to climate warming. In our SGSEN simulations, it appears that the main source of variability between ice sheets with different geometries comes from the interior of the EAIS and the drainage basins of Ninnis and Totten glaciers (Fig. 10). The latter remains thicker in the alternative geometry experiments than in the correspondent CFEN/SSEN correspondent experiment (Figs. 10e-g), whereas the former is thinner in gmt3 (Fig. 10g). Some variability can also be observed in the WAIS domain. Parts of Pine Island Glacier appear to resist ice sheet collapse in the thicker-ice-geometry experiments (i.e., gmt2 and gmt3) when compared to the CFEN/SSEN correspondent run (Figs. 10f,g). Given the observed spread, the three ensemble members constrain the range of potential sea level contributions from Antarctica during the MIS11c highstand at 405 ka to 2.3–8.8 m (minimum from Vostok, maximum from EDC$_{\mathrm{Hol,LGMavg}}$).

https://doi.org/10.5194/tc-2020-112
Preprint. Discussion started: 25 May 2020

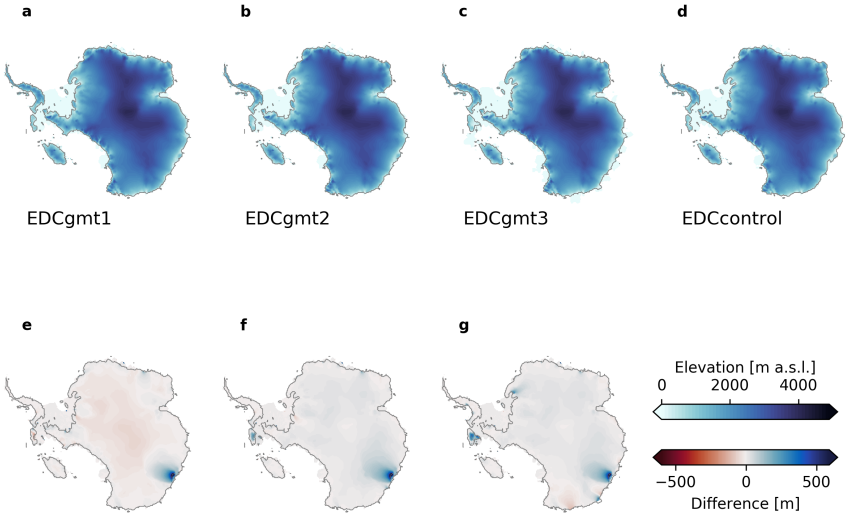

Figure 10. EDC-forced SGSEN members at 405 ka. (a-c) the different geometries corresponding to gmt1-3; (d) their reference run. i.e., CFEN member forced by the EDC-derived GI. (e-g) difference maps between their reference (panel d) and the three resulting ice sheet geometries (respectively panels a-c).

4 Discussion

Offshore and far-field studies show results similar to our model-based inferences regarding the loss of the WAIS during MIS11c and minor losses of ice from the EAIS (thinning and margin retreat). Sediment cores in the WAIS sector of the Southern Ocean revealed evidence for a strong ice retreat during MIS11 (e.g., Scherer et al., 1998), whereas evidence for the EAIS retreat over past Quaternary interglacials has only recently been provided (Wilson et al., 2018, core U1361 in Fig. 1). Hillenbrand et al. (2009) compared sediment cores PS2547 and PS58/254 from the WAIS sector, and PS1506 offshore of Dronning Maud Land (Fig. 1) and found them to be inconclusive regarding the evidence for a WAIS collapse during MIS11, suggesting MIS13 or MIS15 as more likely candidates. They postulated, however, that the duration is more important than the magnitude of warming for a WAIS drawdown. Scherer et al. (1998) argue, based on samples from sediment cores drilled below Ice Stream B, that open ocean conditions existed for the Ross Ice Shelf Basin during MIS11. This is consistent with the open-ocean conditions required to explain a closer source of moisture fuelling an advance of Dry Valley glaciers during the same period (Swanger et al., 2017). Finally, Raymo and Mitrovica (2012) estimated a MIS11 sea level rise of 6 to 13 m above PD, which they postulate

https://doi.org/10.5194/tc-2020-112
Preprint. Discussion started: 25 May 2020

that, considering the upper bound, could only be obtained if, in addition to Greenland's contribution, the WAIS had collapsed and the EAIS also provided its share.

Numerical modelling studies in which the WAIS did not collapse during MIS11 were acknowledged to be less sensitive to the ability of ocean temperatures to drive basal melting (e.g., Pollard and DeConto, 2009; Tigchelaar et al., 2019). Despite differences in the sensitivity to ocean temperature, our results support those of Tigchelaar et al. (2019) and Albrecht et al. (2020) regarding the minor role that variations in sea level alone play in driving ice sheet retreat. Instead, changes in sea level most likely act to boost the effect of air and ocean temperatures to drive the ice loss, as stipulated by Tigchelaar et al. (2019). In their study, Pollard and DeConto (2009) use the LR04 stack as forcing, which lacks significant warming above PI during MIS11c, and for which we did not obtain a WAIS collapse either, despite the very different approaches in reconstructing the transient signal between the two studies.

We found that the relatively low temporal resolution of LR04 is not the reason why it cannot produce a WAIS collapse as do the ice core records (i.e., it would have missed a short period where a pronounced peak would be present). Our RSEN low-pass-filter-forcing experiments with the EDC GI reconstruction show a WAIS collapse and significant ice sheet contraction, regardless of how much high-frequency variability is removed. It is worth reminding that the LR04 stack contains no regional signal from the Southern Ocean at all, with its southernmost oxygen isotope records being taken from cores drilled in the Agulhas region (south of Africa in the Atlantic Ocean), at about 45°S (see Fig. 1 in Lisiecki and Raymo, 2005). This could explain why LR04 does not capture the Antarctic warming event during MIS11, and consequently fails to provoke ice sheet contraction. The different criteria attempted for its scaling also had little effect (Fig. 6), further strengthening our argument that LR04 shows the global signature of MIS11c, which is not representative of the peak warming in Antarctica. A possible way of circumventing this problem could be by using a similar approach to Sutter et al. (2019), who combined the LR04 stack and EDC ice-core temperature records, that led to a WAIS collapse during MIS11.

From our experiments with different initial ice sheet geometries it seems that ice-shelf calving plays a role just as big as, if not larger, than basal ice-shelf melting in terms of regulating the grounding line advance, since in gmt3 the grounding lines advanced more than in gmt2. The simplified treatment of the grounding lines could also have had an influence on the seeming insensitivity of our experiments to sea level uncertainties, although models which apply more refined treatments yield similar results for a similar spatial resolution (e.g., Tigchelaar et al., 2019). Thus, while these caveats must be taken into consideration, they do not appear to have influenced our results dramatically, since they can be directly compared to what other studies have obtained using similar forcings.

To construct our climate forcings, we used four different proxy records which show significant differences in their structure during the peak warming. They either consist of a short single peak (Vostok), or a prolonged period of (relatively) warmer conditions, including a peak (LR04, DF, and EDC). Although the extensive warming signal is seen in most records, they too show differences from one another. For example, EDC and DF, which are the most similar among the four records, start shifting to their warmest conditions at about the same time (ca 414 ka), but peak at different times. DF peaks at 410 ka, which is 3 kyr earlier than EDC. However, the WAIS collapse occurs at 407 ka for the DF and at 406 ka for the EDC core experiments, which is closer than the timing of their peak warming. Both records also produce similar ice volumes (Fig. 9) and extents

https://doi.org/10.5194/tc-2020-112
Preprint. Discussion started: 25 May 2020

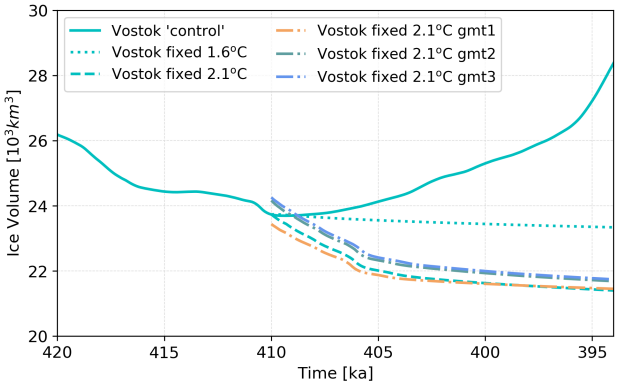

Figure 11. Sensitivity of the AIS ice volume ($10^3 \mathrm{km}^3$) to "post 410 ka constant conditions". Solid line shows ice-sheet volume for the Vostok-forced CFEN member (c.f. Fig. 4), dotted and dashed lines show ice-sheet volume history when conditions are kept constant using a GI correspondent to 1.6°C and 2.1°C above PI, respectively.

(Supplementary Fig. S4). In contrast, the Vostok-forced ensemble member, which has a short warming peak, shows no collapse of the WAIS despite having a short warming peak of a similar GI magnitude at 410 ka.

It is important to remember that the discrepancies in the time of the peak warming and ice sheet collapse are within the uncertainty in the age models of the ice cores (Parrenin et al., 2007; Bazin et al., 2013), preventing us from establishing an exact point in time for these events. It should also be mentioned that the combination of GI and climate-model forcing to reconstruct the surface temperature results in a warmer temperature signal than the one obtained directly from the δD of the EDC and DF ice cores. This happens both to the average over the entire domain and at their drilling sites (Fig. 11), highlighting the fact that a linear interpolation between two fields does not fully capture the spatial pattern of the temperature anomalies. The EDC and DF δD-derived temperatures peak at 3.1 and 2.7°C respectively, while the temperature obtained by the GI reconstruction (Eq. 2) ranges from 3.3 to 3.7°C. The same does not hold for Vostok: the δD-derived temperature peaks at 2.1°C, compared to the GI reconstruction that peaks at 1.6°C at the Vostok drilling site, and 2.5°C averaged over the entire domain. This mismatch between isotope-derived and GI-derived temperatures does not make our results less relevant: a set of simulations where the GI was kept constant at its 410 ka peak value (at 2.1°C above PI, i.e., the peak warming of Vostok) from 410 ka onward resulted in a WAIS collapse for all starting geometries after ca. 4 kyr (with a total sea-level contribution of 6.5–8.0 m at 405 ka; Fig. 11), coinciding with what is observed for the EDC and DF-forced experiments. Thus, a more prolonged warming as seen in DF (which has a GI peak of similar magnitude as Vostok) and EDC seems to be crucial for the collapse of the WAIS, as opposed to the intensity of such peak, similar to what was suggested by Robinson et al. (2017) for the GIS.

Considering that EDC, Vostok, and DF reach similar GI values at 411 ka (Fig. 4a), the value at this point seems to be the threshold for which a WAIS collapse is possible if such conditions are sustained for at least 4–5 kyr. This happens *before* the peak warming in these records, and corresponds to a 1.6–2.1°C mean-annual atmospheric warming across the Antarctic

https://doi.org/10.5194/tc-2020-112
Preprint. Discussion started: 25 May 2020

continent (i.e., the range of resulting temperature values between the three GI reconstructions cited above; Fig. S6), which, considering our ocean forcing, translates to a 1.5–1.9°C warming of the ocean surface averaged around Antarctica (i.e., south of 65°S). This threshold is much lower than the 4° C stipulated by Tigchelaar et al. (2018), but is in line with model results from Turney et al. (2020) for the LIG. Our surface ocean temperature threshold should be considered with caution, because it is derived using an interpolation of ocean temperatures to compute our anomalies instead of a coupled ice-ocean setup (a full description is available in the supplementary material). A simulation analogous to the one where the GI was kept fixed at conditions equivalent to the peak warming of Vostok, but using the GI value that corresponds to a 1.6°C warming across Antarctica for the Vostok ice core, was performed (Fig. 11). This time, a WAIS collapse has not been observed, corroborating the lower end of the inferred temperature interval. It should be noted that the duration of the warming as the key factor for the WAIS collapse is specific to MIS11c. In other words, a more intense albeit shorter peak warming could also trigger WAIS collapse, since a strong rate of warming can drive ice retreat at a much faster pace, which was most likely the case for the LIG (Dutton et al., 2015; Turney et al., 2020).

The EDC and DF GI reconstructions yield results that mirror expectations from the paleorecord, including the estimations of the sea level contribution from Antarctica. While Robinson et al. (2017) found that Greenland contributed between 3.9 and 7.0 m to sea level rise (having 6.1 m s.l.e. as the most likely value), the time at which their sea level contribution curve peaks, the uncertainties in the age models of the different analysed ice cores (Petit et al., 1999; Parrenin et al., 2007; Bazin et al., 2013), and the suggested asynchronicity between the GIS and AIS minimum extents (Steig and Alley, 2002), do not allow us to simply constrain Antarctica's contribution by subtracting Greenland's contribution from the global sea level highstand. Based on EDC and DF (i.e., the scenarios where the WAIS collapsed), our interval for the potential sea level contribution of the AIS is 6.4–8.8 m, with the largest source of uncertainty being the contribution of the EAIS (Fig. 12). Contrary to the WAIS (4.3–4.6 m s.l.e.), the EAIS reacted sensitively to the choice of starting ice geometry - especially over Wilkes Land, which remains stable given a more extensive ice sheet. Conversely, a more extensive yet thinner ice sheet than the reference control run (i.e., gmt1; Fig. 3, Table 3) proved to be more prone to ice loss over the rest of the AIS than the relatively "bulkier" ice sheet of the control run (Fig. 12). This yields a range of 2.4 to 4.2 m s.l.e. contribution of the EAIS at 405 ka.

5 Conclusions

Several studies have been carried out trying to reconstruct past ice changes over the Antarctic continent, but to our knowledge no special focus has been given to Antarctica's response to the peak warming during MIS11c and the driving mechanisms behind it. To fill this gap we evaluated the deglaciation of Antarctica using a numerical ice-sheet model forced by a combination of climate model time-slice-forcing and various transient signals. These signals were obtained from ice cores taken at the EAIS interior and a stacked record of deep-sea sediment cores taken from far-field regions. We evaluated possible sources of uncertainty due to (i) the scaling of the GI, (ii) multi-centennial variability and temporal record resolution, (iii) different sea level reconstructions, and (iv) initial ice-sheet conditions. While sea level, higher-frequency variability, and the GI scaling of the records seemed to play a small role, different responses were seen for both East and West Antarctic Ice Sheets regarding the

https://doi.org/10.5194/tc-2020-112
Preprint. Discussion started: 25 May 2020

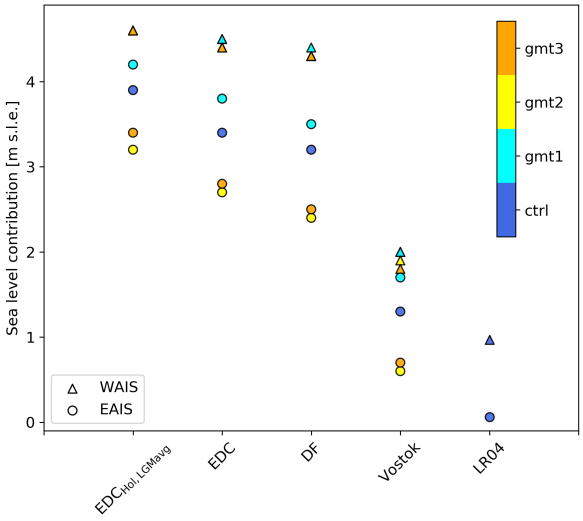

Figure 12. Sea level contribution (in m s.l.e.) of each SGSEN member during the global sea level highstand at 405 ka. LR04 member from CFEN is included for reference.

different applied transient signals, and for the initial ice sheet configurations. Among the applied ice-core reconstructions, the warming captured by the Vostok ice core during MIS11c was not strong enough to cause a collapse of the WAIS, which was attributed to the short duration of its peak. Our results indicate that WAIS collapse was caused by the duration rather than the intensity of warming, and that it was insensitive to the choice of the starting geometry. The latter proved to be a larger source of uncertainty for the EAIS. Regarding the initial questions posed in the beginning of this study, we now provide objective, short answers to them:

1. **How did the AIS respond to the peak warming of MIS11c? What are the uncertainties in the AIS minimum configuration, its timing and potential sea level contribution?**
   We found the WAIS to collapse about 5 kyr after the mean-annual atmospheric temperature exceeded 1.6–2.1°C above Pre Industrial across Antarctica. Some ice loss was also observed in marine-based regions of the EAIS. While the contribution to sea level rise by the WAIS was consistent among the experiments for which we observe strong WAIS retreat (4.3–4.6 m), varying mostly due to the choice of climate forcing, the EAIS contribution was less constrained (2.4–4.2 m) because of its sensitivity to the initial geometry of the ice sheet.

2. **What was the main driver for AIS changes in size? Was it warming length, peak temperature, or changes in precipitation? Are any of these processes relevant to future changes in the southern high latitudes?**
   Ice retreat was found to be mostly sensitive to the length of warming rather than its intensity. We found a threshold of 1.6–2.1°C above PI mean-annual average atmospheric temperatures at which strong WAIS ice retreat is triggered given

https://doi.org/10.5194/tc-2020-112
Preprint. Discussion started: 25 May 2020

a 4–5 kyr duration of the warming. This indicates that an onset of massive WAIS retreat in the near future is possible, although aiming at a reduction in global/Antarctic average temperatures could still prevent its collapse.

Code and data availability. The numerical code for the ice-sheet model SICOPOLIS can be obtained in http://sicopolis.net/. All settings files used for the model runs are available in https://github.com/martimmas/MIS11c_exps

Author contributions. IR idealised the study. IR, JB, and MMB designed the experiments, and MMB and JB carried them out. MMB and JB analysed the results. MP provided the climate forcing. MMB prepared the manuscript with contributions from all co-authors.

Competing interests. The authors declare that they have no conflict of interest.

Acknowledgements. This work is funded by the MAGIC-DML project. MAGIC-DML is a consortium supported by Stockholm University (Arjen Stroeven), Norwegian Polar Institute/NARE under Grant "MAGIC-DML" (Ola Fredin), the US National Science Foundation under Grant No. PLR-1542930 (Jonathan Harbor & Nathaniel Lifton), Swedish Research Council under Grant No. 2016-04422 (Jonathan Harbor & Arjen Stroeven), and the German Research Foundation (DFG) Priority Programme 1158 "Antarctic Research" under Grant No. 365737614 (Irina Rogozhina & Matthias Prange). Jorge Bernales has been supported by the MAGIC-DML project through DFG SPP 1158 (RO 4262/1-6). We would also like to acknowledge support from the Carl Mannerfelts fond and the Bolin Centre Climate Research School (Martim Mas e Braga). The ice-sheet model simulations were performed on the GeoMod cluster at MARUM, Bremen University. We thank Andreas Manschke and the GeoMod team at MARUM, Bremen University, for providing us with continuous access to their computer cluster where the model simulations were performed.

https://doi.org/10.5194/tc-2020-112
Preprint. Discussion started: 25 May 2020

References

Albrecht, T., Winkelmann, R., and Levermann, A.: Glacial-cycle simulations of the Antarctic Ice Sheet with the Parallel Ice Sheet Model (PISM) – Part 1: Boundary conditions and climatic forcing, The Cryosphere, 14, 599–632, https://doi.org/10.5194/tc-14-599-2020, 2020.

Bazin, L., Landais, A., Lemieux-Dudon, B., Kele, H. T. M., Veres, D., Parrenin, F., Martinerie, P., Ritz, C., Capron, E., Lipenkov, V., et al.: An optimized multi-proxy, multi-site Antarctic ice and gas orbital chronology (AICC2012): 120-800 ka, Climate of the Past, 9, 1715–1731, 2013.

Beckmann, A. and Goosse, H.: A parameterization of ice shelf–ocean interaction for climate models, Ocean modelling, 5, 157–170, 2003.

Berger, A. and Loutre, M.-F.: Climate 400,000 years ago, a key to the future?, Washington DC American Geophysical Union Geophysical Monograph Series, 137, 17–26, 2003.

Bernales, J., Rogozhina, I., Greve, R., and Thomas, M.: Comparison of hybrid schemes for the combination of shallow approximations in numerical simulations of the Antarctic Ice Sheet, The Cryosphere, 11, 247–265, https://doi.org/10.5194/tc-11-247-2017, 2017a.

Bernales, J., Rogozhina, I., and Thomas, M.: Melting and freezing under Antarctic ice shelves from a combination of ice-sheet modelling and observations, Journal of Glaciology, 63, 731–744, 2017b.

Bintanja, R. and van de Wal, R.: North American ice-sheet dynamics and the onset of 100,000-year glacial cycles, Nature, 454, 869–872, 2008.

Capron, E., Rovere, A., Austermann, J., Axford, Y., Barlow, N. L., Carlson, A. E., de Vernal, A., Dutton, A., Kopp, R. E., McManus, J. F., et al.: Challenges and research priorities to understand interactions between climate, ice sheets and global mean sea level during past interglacials, Quaternary Science Reviews, 219, 308–311, 2019.

Clark, P. U., Dyke, A. S., Shakun, J. D., Carlson, A. E., Clark, J., Wohlfarth, B., Mitrovica, J. X., Hostetler, S. W., and McCabe, A. M.: The Last Glacial Maximum, Science, 325, 710–714, https://doi.org/10.1126/science.1172873, 2009.

Clason, C. C., Applegate, P., and Holmlund, P.: Modelling Late Weichselian evolution of the Eurasian ice sheets forced by surface meltwater-enhanced basal sliding, Journal of Glaciology, 60, 29–40, 2014.

de Boer, B., van de Wal, R. S. W., Lourens, L. J., Bintanja, R., and Reerink, T. J.: A continuous simulation of global ice volume over the past 1 million years with 3-D ice-sheet models, Climate Dynamics, 41, 1365–1384, https://doi.org/10.1007/s00382-012-1562-2, 2013.

Dolan, A. M., De Boer, B., Bernales, J., Hill, D. J., and Haywood, A. M.: High climate model dependency of Pliocene Antarctic ice-sheet predictions, Nature communications, 9, 2799, 2018.

Dutton, A., Carlson, A. E., Long, A. J., Milne, G. A., Clark, P. U., DeConto, R., Horton, B. P., Rahmstorf, S., and Raymo, M. E.: Sea-level rise due to polar ice-sheet mass loss during past warm periods, Science, 349, aaa4019, https://doi.org/10.1126/science.aaa4019, 2015.

EPICA Community Members: Eight glacial cycles from an Antarctic ice core, Nature, 429, 623–628, https://doi.org/10.1038/nature02599, 2004.

Favier, L., Jourdain, N. C., Jenkins, A., Merino, N., Durand, G., Gagliardini, O., Gillet-Chaulet, F., and Mathiot, P.: Assessment of sub-shelf melting parameterisations using the ocean–ice-sheet coupled model NEMO (v3. 6)–Elmer/Ice (v8. 3), Geoscientific Model Development, 12, 2255–2283, 2019.

Forsström, P.-L. and Greve, R.: Simulation of the Eurasian ice sheet dynamics during the last glaciation, Global and Planetary Change, 42, 59–81, 2004.

Forsström, P.-L., Sallasmaa, O., Greve, R., and Zwinger, T.: Simulation of fast-flow features of the Fennoscandian ice sheet during the Last Glacial Maximum, Annals of Glaciology, 37, 383–389, 2003.

https://doi.org/10.5194/tc-2020-112
Preprint. Discussion started: 25 May 2020

Greve, R.: Application of a polythermal three-dimensional ice sheet model to the Greenland ice sheet: response to steady-state and transient climate scenarios, Journal of Climate, 10, 901–918, 1997.

Greve, R.: Relation of measured basal temperatures and the spatial distribution of the geothermal heat flux for the Greenland Ice Sheet, Annals of Glaciology, 42, 424–432, 2005.

Greve, R. and Blatter, H.: Comparison of thermodynamics solvers in the polythermal ice sheet model SICOPOLIS, Polar Science, 10, 11–23, 2016.

Handiani, D., Paul, A., Prange, M., Merkel, U., Dupont, L., and Zhang, X.: Tropical vegetation response to Heinrich Event 1 as simulated with the UVic ESCM and CCSM3, Climate of the Past, 9, 1683–1696, 2013.

Hearty, P. J., Hollin, J. T., Neumann, A. C., O'Leary, M. J., and McCulloch, M.: Global sea-level fluctuations during the Last Interglaciation (MIS 5e), Quaternary Science Reviews, 26, 2090–2112, 2007.

Hillenbrand, C.-D., Fütterer, D., Grobe, H., and Frederichs, T.: No evidence for a Pleistocene collapse of the West Antarctic Ice Sheet from continental margin sediments recovered in the Amundsen Sea, Geo-Marine Letters, 22, 51–59, https://doi.org/10.1007/s00367-002-0097-7, http://link.springer.com/10.1007/s00367-002-0097-7, 2002.

Hillenbrand, C.-D., Kuhn, G., and Frederichs, T.: Record of a Mid-Pleistocene depositional anomaly in West Antarctic continental margin sediments: an indicator for ice-sheet collapse?, Quaternary Science Reviews, 28, 1147–1159, https://doi.org/10.1016/j.quascirev.2008.12.010, 2009.

Hodell, D. A., Charles, C. D., and Ninnemann, U. S.: Comparison of interglacial stages in the South Atlantic sector of the Southern Ocean for the past 450 kyr: implications for Marine Isotope Stage MIS11, Global and Planetary Change, 24, 7–26, 2000.

Holden, P. B., Edwards, N. R., Wolff, E. W., Valdes, P. J., and Singarayer, J. S.: The Mid-Brunhes Event and West Antarctic Ice Sheet stability, Journal of Quaternary Science, 26, 474–477, https://doi.org/10.1002/jqs.1525, http://doi.wiley.com/10.1002/jqs.1525, 2011.

Holland, P. R., Jenkins, A., and Holland, D. M.: The response of ice shelf basal melting to variations in ocean temperature, Journal of Climate, 21, 2558–2572, 2008.

Imbrie, J., McIntyre, A., and Mix, A.: Oceanic Response to Orbital Forcing in the Late Quaternary: Observational and Experimental Strategies, in: Climate and Geo-Sciences, edited by Berger, A., Schneider, S., and Duplessy, J. C., pp. 121–164, Springer Netherlands, Dordrecht, https://doi.org/10.1007/978-94-009-2446-8_7, http://link.springer.com/10.1007/978-94-009-2446-8_7, 1989.

Jouzel, J., Masson-Delmotte, V., Cattani, O., Dreyfus, G., Falourd, S., Hoffmann, G., Minster, B., Nouet, J., Barnola, J.-M., Chappellaz, J., et al.: Orbital and millennial Antarctic climate variability over the past 800,000 years, Science, 317, 793–796, 2007.

Kleinen, T., Hildebrandt, S., Prange, M., Rachmayani, R., Müller, S., Bezrukova, E., Brovkin, V., and Tarasov, P. E.: The climate and vegetation of Marine Isotope Stage 11–model results and proxy-based reconstructions at global and regional scale, Quaternary International, 348, 247–265, https://doi.org/10.1016/j.quaint.2013.12.028, 2014.

Kukla, G.: How long and how stable was the last interglacial?, Quaternary Science Reviews, 16, 605–612, https://doi.org/10.1016/S0277-3791(96)00114-X, 1997.

Lisiecki, L. E. and Raymo, M. E.: A Pliocene-Pleistocene stack of 57 globally distributed benthic δ^{18}O records, Paleoceanography, 20, PA1003, https://doi.org/10.1029/2004PA001071, 2005.

Loutre, M. and Berger, A.: Marine Isotope Stage 11 as an analogue for the present interglacial, Global and Planetary Change, 36, 209–217, https://doi.org/10.1016/S0921-8181(02)00186-8, 2003.

Martin, M. A., Winkelmann, R., Haseloff, M., Albrecht, T., Bueler, E., Khroulev, C., and Levermann, A.: The Potsdam Parallel Ice Sheet Model (PISM-PIK)–Part 2: Dynamic equilibrium simulation of the Antarctic Ice Sheet, The Cryosphere, 5, 727–740, 2011.

https://doi.org/10.5194/tc-2020-112
Preprint. Discussion started: 25 May 2020

Milker, Y., Rachmayani, R., Weinkauf, M. F. G., Prange, M., Raitzsch, M., Schulz, M., and Kučera, M.: Global and regional sea surface temperature trends during Marine Isotope Stage 11, Climate of the Past, 9, 2231–2252, https://doi.org/10.5194/cp-9-2231-2013, 2013.

Naish, T., Powell, R., Levy, R., Wilson, G., Scherer, R., Talarico, F., Krissek, L., Niessen, F., Pompilio, M., Wilson, T., et al.: Obliquity-paced Pliocene West Antarctic ice sheet oscillations, Nature, 458, 322–328, 2009.

Parrenin, F., Barnola, J.-M., Beer, J., Blunier, T., Castellano, E., Chappellaz, J., Dreyfus, G., Fischer, H., Fujita, S., Jouzel, J., et al.: The EDC3 chronology for the EPICA Dome C ice core, Climate of the Past, 3, 485–497, 2007.

Petit, J., Jouzel, J., Raynaud, D., Barkov, N., Barnola, J., Basile, I., Bender, M., Chappellaz, J., Davis, J., Delaygue, G., et al.: Vostok ice core data for 420,000 years, IGBP pages/world data center for paleoclimatology data contribution series #2001–076, NOAA/NGDC Paleoclimatology Program, Boulder CO, USA, 2001.

Petit, J.-R., Jouzel, J., Raynaud, D., Barkov, N. I., Barnola, J.-M., Basile, I., Bender, M., Chappellaz, J., Davis, M., Delaygue, G., et al.: Climate and atmospheric history of the past 420,000 years from the Vostok ice core, Antarctica, Nature, 399, 429–436, 1999.

Pollard, D. and DeConto, R.: Description of a hybrid ice sheet-shelf model, and application to Antarctica, Geoscientific Model Development, 5, 1273–1295, 2012.

Pollard, D. and DeConto, R. M.: Modelling West Antarctic Ice Sheet growth and collapse through the past five million years, Nature, 458, 329–332, 2009.

Rachmayani, R., Prange, M., and Schulz, M.: Intra-interglacial climate variability: model simulations of Marine Isotope Stages 1, 5, 11, 13, and 15, Climate of the Past, 12, 677–695, https://doi.org/10.5194/cp-12-677-2016, 2016.

Rachmayani, R., Prange, M., Lunt, D. J., Stone, E. J., and Schulz, M.: Sensitivity of the Greenland Ice Sheet to Interglacial Climate Forcing: MIS 5e Versus MIS 11, Paleoceanography, 32, 1089–1101, https://doi.org/10.1002/2017PA003149, http://doi.wiley.com/10.1002/2017PA003149, 2017.

Raymo, M. E. and Mitrovica, J. X.: Collapse of polar ice sheets during the stage 11 interglacial, Nature, 483, 453–456, https://doi.org/10.1038/nature10891, 2012.

Raynaud, D., Barnola, J.-M., Souchez, R., Lorrain, R., Petit, J.-R., Duval, P., and Lipenkov, V. Y.: The record for Marine Isotopic Stage 11, Nature Communications, 436, 39–40, https://doi.org/10.1038/43639b, 2005.

Reyes, A. V., Carlson, A. E., Beard, B. L., Hatfield, R. G., Stoner, J. S., Winsor, K., Welke, B., and Ullman, D. J.: South Greenland ice-sheet collapse during Marine Isotope Stage 11, Nature, 510, 525–528, https://doi.org/10.1038/nature13456, 2014.

Robinson, A., Alvarez-Solas, J., Calov, R., Ganopolski, A., and Montoya, M.: MIS-11 duration key to disappearance of the Greenland Ice Sheet, Nature Communications, 8, 16 008, https://doi.org/10.1038/ncomms16008, 2017.

Sato, T. and Greve, R.: Sensitivity experiments for the Antarctic Ice Sheet with varied sub-ice-shelf melting rates, Annals of Glaciology, 53, 221–228, 2012.

Scherer, R. P.: Quaternary interglacials and the West Antarctic Ice Sheet, in: Geophysical Monograph Series, edited by Droxler, A. W., Poore, R. Z., and Burckle, L. H., vol. 137, pp. 103–112, American Geophysical Union, Washington, D. C., https://doi.org/10.1029/137GM08, 2003.

Scherer, R. P., Aldahan, A., Tulaczyk, S., Possnert, G., Engelhardt, H., and Kamb, B.: Pleistocene collapse of the West Antarctic Ice Sheet, Science, 281, 82–85, 1998.

Shackleton, N. J., Sánchez-Goñi, M. F., Pailler, D., and Lancelot, Y.: Marine isotope substage 5e and the Eemian interglacial, Global and Planetary change, 36, 151–155, 2003.

Spratt, R. M. and Lisiecki, L. E.: A Late Pleistocene sea level stack, Climate of the Past, 12, 1079–1092, 2016.

https://doi.org/10.5194/tc-2020-112
Preprint. Discussion started: 25 May 2020

Steig, E. J. and Alley, R. B.: Phase relationships between Antarctic and Greenland climate records, Annals of Glaciology, 35, 451–456, 2002.

Sutter, J., Fischer, H., Grosfeld, K., Karlsson, N. B., Kleiner, T., van Liefferinge, B., and Eisen, O.: Modelling the Antarctic Ice Sheet across the mid-Pleistocene transition–implications for Oldest Ice, The Cryosphere, 13, 2023–2041, 2019.

Swanger, K. M., Lamp, J. L., Winckler, G., Schaefer, J. M., and Marchant, D. R.: Glacier advance during Marine Isotope Stage 11 in the McMurdo dry valleys of Antarctica, Scientific reports, 7, 41 433, 2017.

Tigchelaar, M., Timmermann, A., Pollard, D., Friedrich, T., and Heinemann, M.: Local insolation changes enhance Antarctic interglacials: Insights from an 800,000-year ice sheet simulation with transient climate forcing, Earth and Planetary Science Letters, 495, 69–78, https://doi.org/10.1016/j.epsl.2018.05.004, 2018.

Tigchelaar, M., Timmermann, A., Friedrich, T., Heinemann, M., and Pollard, D.: Nonlinear response of the Antarctic Ice Sheet to late Quaternary sea level and climate forcing, The Cryosphere, 13, 2615–2631, 2019.

Turney, C. S., Fogwill, C. J., Golledge, N. R., McKay, N. P., van Sebille, E., Jones, R. T., Etheridge, D., Rubino, M., Thornton, D. P., Davies, S. M., et al.: Early Last Interglacial ocean warming drove substantial ice mass loss from Antarctica, Proceedings of the National Academy of Sciences, 117, 3996–4006, 2020.

Tzedakis, P. C., Wolff, E. W., Skinner, L. C., Brovkin, V., Hodell, D. A., McManus, J. F., and Raynaud, D.: Can we predict the duration of an interglacial?, Climate of the Past, 8, 1473–1485, https://doi.org/10.5194/cp-8-1473-2012, https://www.clim-past.net/8/1473/2012/, 2012.

Uemura, R., Motoyama, H., Masson-Delmotte, V., Jouzel, J., Kawamura, K., Goto-Azuma, K., Fujita, S., Kuramoto, T., Hirabayashi, M., Miyake, T., et al.: Asynchrony between Antarctic temperature and CO2 associated with obliquity over the past 720,000 years, Nature communications, 9, 961, 2018.

Willerslev, E., Cappellini, E., Boomsma, W., Nielsen, R., Hebsgaard, M. B., Brand, T. B., Hofreiter, M., Bunce, M., Poinar, H. N., Dahl-Jensen, D., Johnsen, S., Steffensen, J. P., Bennike, O., Schwenninger, J.-L., Nathan, R., Armitage, S., de Hoog, C.-J., Alfimov, V., Christl, M., Beer, J., Muscheler, R., Barker, J., Sharp, M., Penkman, K. E. H., Haile, J., Taberlet, P., Gilbert, M. T. P., Casoli, A., Campani, E., and Collins, M. J.: Ancient Biomolecules from Deep Ice Cores Reveal a Forested Southern Greenland, Science, 317, 111–114, https://doi.org/10.1126/science.1141758, http://www.sciencemag.org/cgi/doi/10.1126/science.1141758, 2007.

Wilson, D. J., Bertram, R. A., Needham, E. F., van de Flierdt, T., Welsh, K. J., McKay, R. M., Mazumder, A., Riesselman, C. R., Jimenez-Espejo, F. J., and Escutia, C.: Ice loss from the East Antarctic Ice Sheet during late Pleistocene interglacials, Nature, 561, 383–386, https://doi.org/10.1038/s41586-018-0501-8, http://www.nature.com/articles/s41586-018-0501-8, 2018.